Journal of Statistical Physics, Vol. 119, Nos. 3/4, May 2005 (© 2005)
DOI: 10.1007/s10955-005-3768-8

Large Deviation Techniques Applied to Systems with Long-Range Interactions

Julien Barré,[1,2] Freddy Bouchet,[1] Thierry Dauxois,[1] and Stefano Ruffo[1,3]

Received June 16, 2004; accepted February 11, 2005

We discuss a method to solve models with *long-range interactions* in the microcanonical and canonical ensemble. The method closely follows the one introduced by R.S. Ellis, *Physica D* **133**:106 (1999), which uses large deviation techniques. We show how it can be adapted to obtain the solution of a large class of simple models, which can show *ensemble inequivalence*. The model Hamiltonian can have both *discrete* (Ising, Potts) and *continuous* (HMF, Free Electron Laser) state variables. This latter extension gives access to the comparison with dynamics and to the study of non-equilibrium effects. We treat both infinite range and slowly decreasing interactions and, in particular, we present the solution of the α-Ising model in one-dimension with $0 \leqslant \alpha < 1$.

KEY WORDS: long-range interactions; large deviation techniques; mean-field limit.

A system with long-range interactions is characterized by an interparticle potential $V(r)$ which decreases at large distances r slower than a power $r^{-\alpha}$ with $\alpha < d$, d being the dimension of the embedding space.[1] Classical examples are self-gravitating[2] and Coulomb[3] systems, vortices in two-dimensional fluid mechanics,[4] wave-particles interaction[5,6] and trapped charged particles.[7] The behavior of such systems is interesting both from the dynamical point of view, because they display peculiar quasi-stationary states that are related to the underlying Vlasov equations,[8] and from the static point of view, because equilibrium statistical mechanics shows new

[1]Laboratoire de Physique, UMR-CNRS 5672, ENS Lyon, 46 Allée d'Italie, 69364 Lyon cédex 07, France; e-mail: thierry.dauxois@ens-lyon.fr
[2]Theoretical Division, Los Alamos National Laboratory, USA.
[3]Dipartimento di Energetica, "S. Stecco" and CSDC, Università di Firenze, and INFN, via S. Marta, 3, 50139 Firenze, Italy.

types of phase transitions and cases of ensemble inequivalence.[9] In this paper, we will restrict ourselves to the second aspect.

In long-range interacting systems, essentially all the particles contribute to the local field: the fluctuations around the mean value are small because of the law of large numbers. This explains qualitatively why the mean-field scaling, which amounts to let the number of particles go to infinity at fixed volume,[10,11] is usually extremely good. However, let us remind that for long-range interacting systems, microcanonical and canonical ensembles are not necessarily equivalent in the mean-field limit.[12–14] Moreover, because of the non additivity of the energy, the usual construction of the canonical ensemble cannot be applied. This is the reason why the microcanonical ensemble is considered by some authors[2,15] as the only "physically motivated" one. Hence, it is extremely important to develop rigorous techniques to solve non-trivial physical models in the microcanonical ensemble. One finds in books the solution for the perfect gas, but generalizations to interacting particle systems are difficult.

The goal of this paper is to advocate the use of large deviation techniques as a tool to *explicitly* derive microcanonical and canonical equilibrium solutions for a wide class of models. As a first step in this direction, we will discuss here a general solution method to treat in full detail mean-field models without short distance singularity. Large deviation techniques[16,17] are nowadays widely used. For example, Michel and Robert,[18] using these techniques, rigorously derived the statistical mechanics of the two-dimensional Euler equations. The method was later used by Ellis *et al.*[19] to study other two-dimensional geophysical fluids. The statistical mechanics of some models with *discrete* variables has been recently obtained using large deviation theory.[9,20,21] Besides presenting the solution method, we will show in this paper how it can be applied to models whose Hamiltonian depends on *continuous* state variables, like the so-called Hamiltonian Mean-Field (HMF) model[22,23]; the interest being here to obtain solutions in the microcanonical ensemble of models which display a Hamiltonian dynamics, opening the possibility of studying also non-equilibrium effects.

We will first briefly introduce in Section 1 the large deviation technique. In Section 2 we will recall the different steps of the mathematical framework introduced in ref. 19, necessary for a systematic application to long-range interacting systems: we will use the infinite range Potts model as a simple example. In a first instance, we will then treat infinite range models with continuous variables. We will present in Section 3.1 the solution of the HMF model[23] in the microcanonical ensemble and, in the following Section 3.2, we will consider the Colson–Bonifacio model of Free Electron Lasers (FEL),[24] as an example of relevance for physical

applications. In Section 4, we will show that these techniques can be applied also to cases where the interaction is not infinite range but distance dependent; the solution of the so-called α-Ising model,[25] in one dimension with $0 \leqslant \alpha < 1$, will be presented in full detail, allowing us to discuss also the role of boundary conditions. Finally, Section 5 will be devoted to conclusions and perspectives.

1. LARGE DEVIATION THEORY

We will present in this section the main ideas behind large deviation techniques, with an emphasis to applications. For a more rigorous mathematical treatment, we direct the reader to refs. 16 and 17.

1.1. The Large Deviation Principle

Let us consider the sample mean of N independent real random variables X_k with the same distribution and zero average

$$S_N = \frac{1}{N} \sum_{k=1}^{N} X_k. \tag{1}$$

The law of large numbers states that S_N tends toward the average $x = \langle X_k \rangle$, namely 0, when N tends toward infinity. Moreover, if X_k has a finite variance, since all hypotheses of the central limit theorem are fulfilled, the probability distribution $P(\sqrt{N} S_N \in [x, x + dx])$ converges towards a Gaussian, hence the fluctuations of S_N are of order $1/\sqrt{N}$. Typical questions of the large deviation theory are: What is the behavior of the tails of the distribution? What is the probability of a fluctuation of order one of S_N, i.e. what is the value of $P(S_N \in [x, x + dx])$?

Let us be more specific by discussing the usual example of the coin toss. We attribute to heads and tails of a coin the values $X_k = +1$ and $X_k = -1$, respectively. The sum S_N can take $(N+1)$ distinct x-values in the interval $[-1, 1]$. For such values, using simple combinatorial analysis, one easily derives the probability distribution

$$P(S_N = x) = \frac{N!}{\left(\frac{(1+x)N}{2}\right)! \left(\frac{(1-x)N}{2}\right)! \, 2^N}, \tag{2}$$

which, using the Stirling's formula, can be approximated in the large N limit as

$$\ln P(S_N = x) \sim -N \left(\frac{(1+x)}{2} \ln(1+x) + \frac{(1-x)}{2} \ln(1-x) \right) \equiv -N I(x), \tag{3}$$

which defines the function $I(x)$. More precisely, one can prove that for any interval $]x_1,\ x_2[\subset [-1, 1]$,

$$\lim_{N \to \infty} -\frac{1}{N} \ln P(x \in]x_1,\ x_2[) = \max_{x \in]x_1,\ x_2[} I(x). \tag{4}$$

In the language of large deviation theory, one states that S_N fulfills a *large deviation principle*, characterized by the rate function $I(x)$. If one interprets the coin toss experiment as a microscopic realization of a chain of N non-interacting Ising spins, it is straightforward to prove that, in the statistical mechanics vocabulary, $I(x)$ corresponds to the negative of the Boltzmann entropy (divided by the Boltzmann constant) of a state characterized by a fraction x of up-spins. This is a first simple example of the large deviation principle, and the main purpose of this paper is to present other examples of its use for more complicated and physically relevant systems.

1.2. Cramér's Theorem

Cramér's theorem[17] allows one to derive the probability distribution $P(S_N \in [x, x + dx])$ in the large N-limit, providing also a method to compute the rate function $I(x)$. The theorem is formulated for multi-dimensional and identically distributed random variables $X_k \in \mathbb{R}^d$, d being the dimension of the space of the variables. We will formulate the theorem in an informal way, without emphasizing mathematical technicalities.

Let us define the function $\Psi(\lambda)$ as

$$\Psi(\lambda) = \langle e^{\lambda \cdot X} \rangle, \tag{5}$$

where $\lambda \in \mathbb{R}^d$, "$\cdot$" is the usual scalar product and $\langle\ \ \rangle$ is the average over the common probability distribution of the variables X_k. Cramér's theorem states that, if $\Psi(\lambda) < \infty$, $\forall \lambda \in \mathbb{R}^d$, then the sample mean S_N satisfies the large deviation principle

$$\ln P(S_N \in [x, x + \mathrm{d}x]) \sim -N I(x), \tag{6}$$

with rate function $I(x)$ ($x \in \mathbb{R}^d$) given by the Legendre–Fenchel's transform of $\ln \Psi$,

$$I(x) = \sup_{\lambda \in \mathbb{R}^d} (\lambda \cdot x - \ln \Psi(\lambda)). \tag{7}$$

The formulation of the theorem is not restricted to discrete random variables: this will be important for our applications.

A heuristic proof of the theorem for the simplest case $X_k \in \mathbb{R}$ goes as follows. The probability of obtaining $S_N = x$, with $d\mu$ the common probability distribution of each variable X_k, is given by

$$P(S_N \in [x, x + \mathrm{d}x]) = \int \prod_{k=1}^{N} \mathrm{d}\mu(X_k)\ \delta(S_N - x). \tag{8}$$

This formula can also be interpreted as the volume of the phase-space $(X_1, \ldots, X_N)$ under the microcanonical constraint that $S_N = x$. Using the Laplace transform of the Dirac's δ-function, one obtains

$$P(S_N \in [x, x + \mathrm{d}x]) = \frac{1}{2\pi i} \int_\Gamma \mathrm{d}\lambda\ \mathrm{e}^{-N\lambda x} \int \prod_{k=1}^{N} \mathrm{d}\mu(X_k)\ \mathrm{e}^{\lambda \sum_{k=1}^{N} X_k}, \tag{9}$$

where Γ is a path on the complex λ-plane going from $-i\infty$ to $+i\infty$, which crosses the real axis at a positive value. Subsequent manipulations of this formula lead to

$$\begin{aligned} P(S_N \in [x, x + \mathrm{d}x]) &= \frac{1}{2\pi i} \int_\Gamma \mathrm{d}\lambda\ \mathrm{e}^{-N\lambda x} \left[\langle \mathrm{e}^{\lambda X} \rangle \right]^N \\ &= \frac{1}{2\pi i} \int_\Gamma \mathrm{d}\lambda\ \mathrm{e}^{-N(\lambda x - \ln \langle \mathrm{e}^{\lambda X} \rangle)} \overset{N \to \infty}{\simeq} \mathrm{e}^{-N I(x)}, \end{aligned} \tag{10}$$

where $I(x)$ is given in formula (7) with $d = 1$. In the last step, a large N saddle-point approximation has been performed.

Most of the results contained in this paper will be obtained using Cramér's theorem, because the statistical variables of the models we will consider are identically distributed in space (mostly on a lattice). In all cases the function $\ln \Psi$ is differentiable, which also fulfils the hypotheses of the Gärtner–Ellis theorem.[17]

2. A GENERAL METHOD

In this Section, we will describe the use of the large deviation method to solve models with long-range interactions. As already mentioned, Michel and Robert[18] successfully used large deviations techniques to rigorously prove the applicability of statistical mechanics to two-dimensional fluid mechanics, proposed earlier.[26,27] Ellis *et al.*[19] have developed and generalized this approach to solve two-dimensional geophysical

systems with long-range interactions. Here, we will adopt Ellis *et al.* approach, emphasizing the different steps in the construction of thermodynamic functions. The method will be exemplified discussing in detail the three-state Potts model with infinite range interactions. This simple example has been recently used as a toy model to illustrate peculiar thermodynamic properties of long-range systems.[28] The diluted three-state Potts model with short-range interactions has also been studied in connection with "small" systems thermodynamics by Gross.[29]

The Hamiltonian of the three-state Potts model is

$$H_N = -\frac{J}{2N} \sum_{i,j=1}^{N} \delta_{S_i,S_j}. \tag{11}$$

The $1/N$ prefactor is introduced in order to keep energy extensive.[30] Each lattice site i is occupied by a spin variable S_i, which assumes three different states a, b, or c. A pair of spins gives a ferromagnetic contribution $-J$ $(J>0)$ to the total energy if they are in the same state, and no contribution otherwise. It is important to stress that the energy sum is extended over *all* pairs (i, j): the interaction is infinite range.

The solution method consists of three steps.

Step 1: Identifying global variables

Let Σ_N be the phase-space of a N-particles system with Hamiltonian

$$H_N : \Sigma_N \to \mathbb{R} \tag{12}$$

and $\omega_N \in \Sigma_N$ be a specific microscopic configuration. The first step of the method consists in associating to every microscopic configuration ω_N, a global (coarse-grained) variable, $\gamma(\omega_N)$. Then, a new Hamiltonian $\widetilde{H}_N$ can be defined

$$H_N(\omega_N) = \widetilde{H}_N(\gamma(\omega_N)) + R_N(\omega_N). \tag{13}$$

If one can neglect $R_N(\omega_N)$ with respect to $\widetilde{H}_N$ in the large N-limit, then the Hamiltonian can be expressed only in terms of the global variables. When considering the above defined infinite range Potts model, the appropriate global variable is

$$\gamma = (n_a, n_b, n_c), \tag{14}$$

where $(n_a, n_b, n_c = 1 - n_a - n_b)$ are the fractions of spins in the three different states a, b, c. In this case, the Hamiltonian expressed in terms of the global variable is

$$\widetilde{H}_N = -\frac{JN}{2}(n_a^2 + n_b^2 + n_c^2), \tag{15}$$

and coincides with the original Hamiltonian H_N even at finite N. In Section 4, we will discuss the α-Ising model, for which R_N does not vanish.

The global variable γ is of finite dimension in our example, but could be of infinite dimension in other cases. For instance, γ could correspond to a local mass density in a gravitational system, or a coarse-grained vorticity density in two-dimensional turbulence.

Although this type on redefinition of the Hamiltonian might appear to be possible in all cases, this is not true. For instance, in the case of short-range interactions, even after defining a local density of a physical quantity (e.g. magnetization), when performing the large N-limit, no general argument exists to neglect R_N. As a consequence, in such a case, the local density (e.g. the local magnetization) is not the appropriate macroscopic variable. However, we will argue that such a procedure is, instead, viable in general for systems with long-range interactions on a lattice. Keeping the lattice spacing finite is important in order to regularize possible short distance singularities.

Step 2: Deriving an entropy functional for the global variables

Because the mean-field variables are not equiprobable, the number of microscopic configurations leading to a given value of γ does depend on γ itself. Then, one can define an entropy functional $s(\gamma)$,

$$s(\gamma) = \lim_{N\to\infty} \frac{1}{N} \ln \Omega_N(\gamma) = -I(\gamma) + \ln \mathcal{N}, \tag{16}$$

where the Boltzmann constant has been set to unity, $\Omega_N(\gamma)$ is the number of microscopic configurations corresponding to a given value of γ, $I(\gamma)$ is the rate function and $\mathcal{N} = \int d\gamma \Omega_N(\gamma)$ is the total number of states. This is where large deviation theory applies; not only in proving that such an entropy functional exists, but also in providing a procedure to derive it explicitly.

If, besides the dynamical variables which contribute to the global ones, the Hamiltonian depends also on a number of variables n_v which is small with respect to N, it is easy to prove that these additional variables contribute to the entropy for a negligible term, proportional to n_v/N.

For the infinite range Potts model, it is possible to derive the entropy functional $s(\gamma)$ directly, using combinatorial arguments and the Stirling approximation in the large N-limit. However, let us follow instead the procedure given by Cramér's theorem as explained in Section 1.2. Expression (14) for γ, which is identified with x in Section 1.2, can be rewritten as

$$\gamma = \left(\frac{1}{N} \sum_i \delta_{S_i,a}, \frac{1}{N} \sum_i \delta_{S_i,b}, \frac{1}{N} \sum_i \delta_{S_i,c} \right). \tag{17}$$

The local random variables with common probability distribution are here

$$X_k = \left(\delta_{S_k,a}, \delta_{S_k,b}, \delta_{S_k,c} \right). \tag{18}$$

Hence, the generating function Ψ is given by

$$\Psi(\lambda_a, \lambda_b, \lambda_c) = \frac{1}{3} \sum_{S=a,b,c} \left(\mathrm{e}^{\lambda_a \delta_{S,a} + \lambda_b \delta_{S,b} + \lambda_c \delta_{S,c}} \right) \tag{19}$$

$$= \frac{1}{3} \left(\mathrm{e}^{\lambda_a} + \mathrm{e}^{\lambda_b} + \mathrm{e}^{\lambda_c} \right). \tag{20}$$

The large deviation functional is

$$I(\gamma) = \sup_{\lambda_a, \lambda_b, \lambda_c} \left(\lambda_a n_a + \lambda_b n_b + \lambda_c n_c - \ln \Psi(\lambda_a, \lambda_b, \lambda_c) \right). \tag{21}$$

This variational problem can be solved exactly, giving $\lambda_\ell = \ln n_\ell$ with $\ell = a, b, c$. Hence,

$$I(\gamma) = n_a \ln n_a + n_b \ln n_b + (1 - n_a - n_b) \ln(1 - n_a - n_b) + \ln 3. \tag{22}$$

Thermodynamic entropy density is given by $s(\gamma) = -I(\gamma) + \ln \mathcal{N}$, where the normalization factor is $\mathcal{N} = 3$ for the Potts model example, which recovers the result of the combinatorial approach.

Step 3: Microcanonical and canonical variational problems

To obtain the entropy as a function of energy density ε, i.e. to solve a model in the microcanonical ensemble, after performing steps 1 and 2 of

the solution method, one has to find the solution of the following variational problem[19]

$$S(\varepsilon) = \sup_{\gamma} (s(\gamma) \mid H(\gamma) = \varepsilon) , \tag{23}$$

where

$$H(\gamma) = \lim_{N \to \infty} \frac{\widetilde{H}_N(\gamma)}{N}. \tag{24}$$

This result is exact but it corresponds also to an "intuitive" mean-field solution. Finally, let us notice that the total entropy density is intensive: there is no difference in this respect with short-range interacting systems. When other conserved quantities exist, they must be taken into account when solving the variational problem in formula (23). Specific examples will be discussed in Sections (3.1) and (3.2).

For the infinite range Potts model (11), the variational problem is

$$S(\varepsilon) = \sup_{n_a, n_b} \Big(-n_a \ln n_a - n_b \ln n_b - (1 - n_a - n_b) \times \ln(1 - n_a - n_b) \; \Big| - \frac{J}{2} \left(n_a^2 + n_b^2 + (1 - n_a - n_b)^2 \right) = \varepsilon \Big). \tag{25}$$

This variational problem can be solved numerically. The microcanonical inverse temperature $\beta(\varepsilon) = \mathrm{d}S/\mathrm{d}\varepsilon$ can then be derived: it is shown in Fig. 1 in the allowed energy range $[-J/2, -J/6]$. Ispolatov and Cohen[28] have obtained the same result by determining the density of states. A negative specific heat region appears in the energy range $[-0.215\, J, -J/6]$.

Let us now consider the canonical ensemble. The partition function, written in terms of the common probability distribution of the phase-space variables, is

$$Z(\beta, N) = \int \prod_{k=1}^{N} \mathrm{d}\mu(X_k)\, \mathrm{e}^{-\beta H_N} \tag{26}$$

where μ is the probability density of X_k. This is not the usual partition function, but differs from it only for a constant factor, which counts the number of states. Let us remark that we have also used the letter β for the microcanonical inverse temperature. We will comment specifically when the microcanonical inverse temperature differs from the canonical one due to ensemble inequivalence.

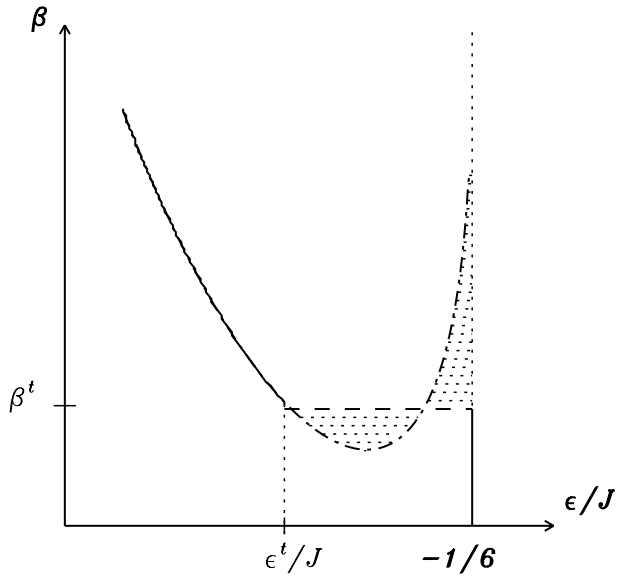

Fig. 1. Caloric curve (inverse temperature versus energy density) of the three states infinite range Potts model. The canonical solution is represented by a solid line. The microcanonical solution coincides with the canonical one for $\varepsilon \leqslant \varepsilon^t$ and is instead indicated by the dash-dotted line for $\varepsilon^t \leqslant \varepsilon < -J/6$. The increasing part of the microcanonical dash-dotted line corresponds to a negative specific heat region. In the canonical ensemble, the model displays a first order phase transition at β^t. The two dotted regions bounded by the dashed line and by the microcanonical dash-dotted line have the same area (Maxwell's construction).

Approximating Hamiltonian H_N in the large N-limit with the one expressed in terms of the global variable γ, one gets

$$Z(\beta, N) \overset{N\to\infty}{\simeq} \frac{\int d\gamma\, \Omega_N(\gamma)\, \mathrm{e}^{-\beta H(\gamma)}}{\int d\gamma\, \Omega_N(\gamma)}. \tag{27}$$

For infinite range models, formula (27) is exact for all N because the rest R_N vanishes. Using formula (16), one obtains

$$Z(\beta, N) \simeq \int d\gamma\ \mathrm{e}^{-N(-s(\gamma)+\beta H(\gamma))}. \tag{28}$$

Applying the saddle point method, the partition function is rewritten as

$$Z(\beta, N) \simeq \mathrm{e}^{-NF(\beta)}, \tag{29}$$

where the "free energy" $F(\beta)$ is obtained solving the variational problem

$$F(\beta) = \inf_{\gamma} (\beta H(\gamma) - s(\gamma)) . \tag{30}$$

Our "free energy" is the usual free energy multiplied by the inverse temperature. This helps because physical states will correspond to minima of such free energy also for negative inverse temperatures.

In the case of the infinite range three-state Potts model, the canonical free energy can be explicitly derived solving the following variational problem

$$F(\beta) = \inf_{n_a, n_b, n_c} \Big(n_a \ln n_a + n_b \ln n_b + n_c \ln n_c - \frac{\beta J}{2} \left(n_a^2 + n_b^2 + n_c^2 \right) | n_a + n_b + n_c = 1 \Big). \tag{31}$$

To obtain the caloric curve, one has to compute $\varepsilon = dF/d\beta$. Figure 1 shows that at the canonical transition inverse temperature $\beta^t \simeq 2.75$, corresponding to the energy $\varepsilon^t/J \simeq -0.255$, a first order phase transition appears, with an associated latent heat. The low energy "magnetized" phase becomes unstable, while the high energy "homogeneous" phase, which has the constant energy density, $\varepsilon/J = -1/6$, is stabilized. In Fig. 1, the two dotted regions have the same area, respecting Maxwell's construction. At the inverse transition temperature, there is also a jump in the global variables (n_a, n_b, n_c) which are the order parameters of the model.

This extremely simple example shows already *ensemble inequivalence*. In the microcanonical ensemble, there is no phase transition and the specific heat becomes negative. On the other hand, in the canonical ensemble, there is a first order phase transition with a latent heat. The caloric curves do not coincide. We observe that in the energy range of ensemble inequivalence, microcanonical temperatures, $(dS/d\varepsilon)^{-1}$, do not coincide with any canonical one.

This is an example of the more general fact that entropy $s(\varepsilon)$ is not always the Legendre–Fenchel transform of the free energy $F(\beta)$. A general discussion of ensemble inequivalence, both at the thermodynamic level and at the level of equilibrium macrostates, is provided in refs. 19 and 21, while a classification of phase transition and of ensemble inequivalence situations is reported in ref. 31.

This concludes the general presentation of the different steps of the method to derive the statistical mechanics of long-range interacting systems.

3. EXAMPLES

In this section, we will discuss the application of the large deviation method to two examples which share the difficulty of computing the entropy for a phase-space with *continuous* variables. When presenting the method, we have discussed in parallel its application to a model with *discrete* variables, the infinite range three-state Potts model, which however could have been solved by direct states counting.[28] This latter approach cannot be used when the variables are continuous. Obtaining microcanonical entropy often implies the solution of too complicated integrals, and indeed one does not find many examples of such solutions in the literature. On the contrary, the large deviation method is not restricted to discrete variables and we will show that it can even be simpler to use in such a case.

3.1. The Hamiltonian Mean Field Model

The Hamiltonian Mean Field (HMF) model[22,23] is defined by the following Hamiltonian

$$H_N = \sum_{i=1}^{N} \frac{p_i^2}{2} + \frac{C}{2N} \sum_{i,j} \cos(\theta_i - \theta_j), \tag{32}$$

where $\theta_i \in [0, 2\pi[$ is the position (angle) of the ith article on a circle and p_i the corresponding conjugate variable. This system can be seen as representing particles moving on a unit circle interacting via an infinite range attractive ($C < 0$) or repulsive ($C > 0$) cosine potential or, alternatively, as classical XY-rotors with infinite range ferromagnetic ($C < 0$) or antiferromagnetic ($C > 0$) couplings. The renormalization factor N of the potential energy is kept not only for historical reasons, but also because it simplifies the derivation of the variational problems and makes the problem well defined. As we will see, this implies that the usual energy per particle and temperature are well defined in the $N \to \infty$ limit. In the literature, some authors have treated the case in which energy is not extensive. This leads to different thermodynamic limit behaviors.[32,33]

The canonical solution of this model has been derived using the Hubbard–Stratonovich transformation.[23] The microcanonical solution has been heuristically obtained, under the hypothesis of concave entropy in ref. 34 and in a different form in ref. 35. In this section, we will derive both solutions with no additional hypothesis. We will verify that the two ensembles give equivalent predictions.

Step 1: Hamiltonian (32) can be rewritten as

$$H_N = \sum_{i=1}^{N} \frac{p_i^2}{2} + \frac{NC}{2}(M_x^2 + M_y^2), \tag{33}$$

where the magnetization is

$$\mathbf{M} = M_x + i M_y = \frac{1}{N} \sum_k \mathrm{e}^{i\theta_k}, \quad \text{with } M = |\mathbf{M}|. \tag{34}$$

By a direct inspection of Hamiltonian (33), one can identify the global quantities $u = \frac{1}{N}\sum_i p_i^2$, M_x and M_y. Moreover, since $v = \frac{1}{N}\sum_i p_i$ is a conserved quantity with respect to the dynamics defined by Hamiltonian (32), it will be included in the global variable. Hence,

$$\gamma = (u, v, M_x, M_y). \tag{35}$$

The Hamiltonian in terms of the global variable is

$$H(\gamma) = \frac{1}{2}(u + CM^2). \tag{36}$$

Step 2: The vector of local variables is $X_k = (p_k^2, p_k, \cos\theta_k, \sin\theta_k)$. The generating function is

$$\Psi(\lambda_u, \lambda_v, \lambda_c, \lambda_s) = \left\langle \mathrm{e}^{\lambda_u p^2 + \lambda_v p + \lambda_c \cos\theta + \lambda_s \sin\theta} \right\rangle \tag{37}$$

$$\sim \mathrm{e}^{-\lambda_v^2/4\lambda_u} \sqrt{\frac{\pi}{-\lambda_u}}\, I_0\left(\sqrt{\lambda_c^2 + \lambda_s^2}\right), \tag{38}$$

where I_0 is the modified Bessel function of order 0. In the last expression, we have not reported the constant factor $\int_\Sigma dp\, d\theta$ which is finite because the domain of integration Σ is bounded due to the finiteness of the energy. The sign $\sim$ indicates that formula (38) is valid only at leading order; indeed, as $\Sigma \neq \mathbb{R} \times [0, 2\pi[$, neither the Gaussian nor the Bessel functions are fully exact.

The large deviation functional is then given, apart from trivial constants, by

$$I(\gamma) = \sup_{\lambda_u,\lambda_v,\lambda_c,\lambda_s} \left[\lambda_u u + \lambda_v v + \lambda_c M_x + \lambda_s M_y - \ln I_0\left(\sqrt{\lambda_c^2+\lambda_s^2}\right) + \frac{\lambda_v^2}{4\lambda_u} + \frac{1}{2}\ln(-\lambda_u) \right]. \quad (39)$$

This variational problem can be solved for the "kinetic" subspace (λ_u, λ_v) separately from the "configurational" one (λ_c, λ_s). The entropy as a function of the global variable is then

$$s(\gamma) = s_{\text{kin}}(u, v) + s_{\text{conf}}(M), \quad (40)$$

where

$$s_{\text{kin}}(u, v) = \frac{1}{2}\ln(u - v^2) + \text{const} \quad (41)$$

$$s_{\text{conf}}(M) = -\sup_{\lambda}[\lambda M - \ln I_0(\lambda)] = -\bar{\lambda}M + \ln I_0(\bar{\lambda}), \quad (42)$$

with $\lambda = \sqrt{\lambda_c^2+\lambda_s^2}$ and $\bar{\lambda}$ the solution of the variational problem in (42). Let us remark that Cauchy–Schwarz inequality implies that $u \geqslant v^2$.

Step 3: It is therefore possible to derive the microcanonical variational problem

$$S(\varepsilon, v) = \sup_{M,u}\left[\frac{1}{2}\ln(u - v^2) + s_{\text{conf}}(M) \,\middle|\, \frac{1}{2}u + \frac{C}{2}M^2 = \varepsilon,\ v = \text{const}\right], \quad (43)$$

and the canonical one

$$F(\beta) = \inf_{M,u,v}\left[\frac{\beta}{2}\left(u + CM^2\right) - \frac{1}{2}\ln(u - v^2) - s_{\text{conf}}(M)\right]. \quad (44)$$

We show here the solution of both variational problems in the case $v = 0$ and $C = -1$, for which a second order phase transition appears. Shifting v to non-vanishing values does not produce anything new, whereas the second order phase transition disappears for positive values of C.

Solving the sup condition in Eq. (42) leads to the consistency equation $M = I_1(\lambda)/I_0(\lambda) \equiv m(\lambda)$, which determines the optimal value of λ, $\bar{\lambda} = m^{-1}(M)$. Using the energy constraint, Eq. (43) can be rewritten as

$$S(\varepsilon) = \sup_{M \in [0,1[} \left[s(M,\varepsilon) = \frac{1}{2} \ln(2\varepsilon + M^2) + s_{\text{conf}}(M) \right]. \tag{45}$$

In order to determine the global maximum of S, let us note that in Eq. (45) M takes values in the interval $[0, 1[$. Moreover, an asymptotic expansion shows that $s(M,\varepsilon) \overset{M\to 1}{\sim} (1/2)\ln(1-M)$, which diverges to $-\infty$ when M tends to 1. Thus, a global maximum of the continuous function s with respect to M exists and is attained inside the interval $[0, 1[$. To determine this maximum one has first to solve the extremal condition

$$\frac{\bar{M}}{2\varepsilon + \bar{M}^2} = -s'_{\text{conf}}(\bar{M}) = m^{-1}\left(\bar{M}\right). \tag{46}$$

The unique solution of this equation is $\bar{M} = 0$ for $\varepsilon > 1/4$, while a non-vanishing magnetization solution bifurcates from it at $\varepsilon = 1/4$, originating the second order phase transition. One can indeed show that

$$s(M,\varepsilon) = \frac{\ln(2\varepsilon)}{2} + \left(\frac{1}{4\varepsilon} - 1\right) M^2 + o\left(M^4\right), \tag{47}$$

which clarifies the stability change at $\varepsilon = 1/4$ of the $\bar{M} = 0$ solution. Formula (47) was also obtained in ref. 36 in connection with the fluctuations of the magnetization.

Let us remark that $(\mathrm{d}S)/(\mathrm{d}\varepsilon)$ is nothing but the inverse of twice the kinetic energy, which is the usual microcanonical temperature. Moreover, condition (46) coincides, as expected, with the consistency relation derived in the canonical ensemble.[23] In Fig. 2, we show the full dependence of the entropy on energy and the graph of the free energy versus the inverse temperature, obtained by solving numerically the consistency equation (46) in the low energy (temperature) range. In Fig. 3, we plot the caloric curve and the dependence of the order parameter on energy: the two ensembles give the same predictions because the entropy is concave.

In Appendix A, we discuss a different way of obtaining the microcanonical solution, which treats the kinetic part of the energy in a more traditional way, like, for instance, in gravitational dynamics.[37] The method showed in this section is of more general applicability.

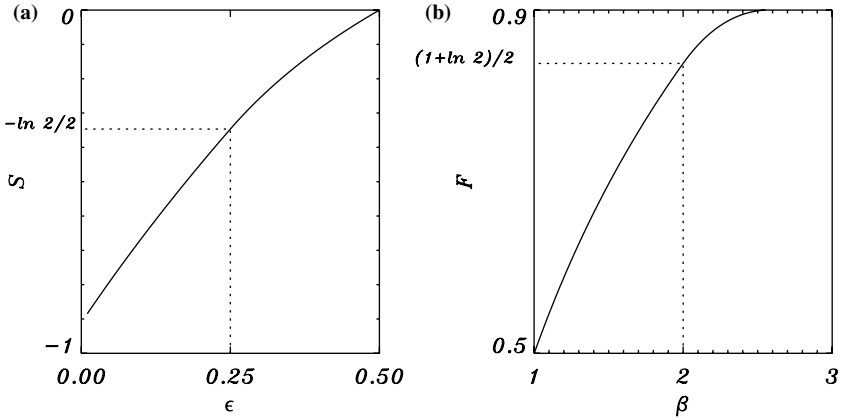

Fig. 2. Entropy versus energy (a) and free energy versus inverse temperature (b) for the HMF model (33) with $C=-1$ and $v=0$. The dotted lines are traced at the phase transition point.

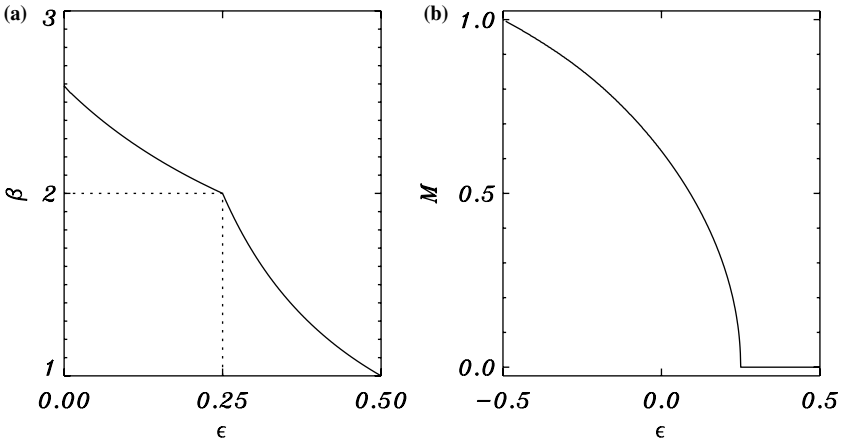

Fig. 3. Inverse temperature versus energy (a) and magnetization versus energy (b) for the HMF model (33) with $C=-1$ and $v=0$. The dotted lines are traced at the phase transition point.

3.2. The Colson–Bonifacio Model for the Free Electron Laser

In the linear Free Electron Laser (FEL), a relativistic electron beam propagates through a spatially periodic magnetic field, interacting with the co-propagating electromagnetic wave; lasing occurs when the electrons bunch in a subluminar beat wave.[24] Scaling away the time dependence of the phenomenon and introducing appropriate variables, it is possible to

catch the essence of the asymptotic state by studying the classical Hamiltonian

$$H_N = \sum_{j=1}^{N} \frac{p_j^2}{2} - N\delta A^2 + 2A \sum_{j=1}^{N} \sin(\theta_j - \varphi). \tag{48}$$

The p_i's represent the velocities relative to the center of mass of the N electrons and the conjugated variables θ_i characterize their positions with respect to the co-propagating wave. The complex electromagnetic field variable, $\mathbf{A} = A\,\mathrm{e}^{i\varphi}$, defines the amplitude and the phase of the dominating mode ($\mathbf{A}$ and $\mathbf{A}^\star$ are conjugate variables). δ is a parameter which measures the average deviation from the resonance condition. In addition to the "energy" H, the total momentum $P = \sum_j p_j + NA^2$ is also a conserved quantity. Most of the studies of this model have concentrated on the numerical solution of Hamiltonian (48), starting from initial states with a small field A and the electrons uniformly distributed with a small kinetic energy. Then, the growth of the field has been observed and its asymptotic value determined from the numerics. Our study below allows to find the asymptotic value of the field analytically.

Step 1: Similarly to the HMF case, Hamiltonian (48) can be rewritten as

$$H_N \simeq N H(\gamma) = N\left(\frac{u}{2} - \delta A^2 + 2A\left(-M_x \sin\varphi + M_y \cos\varphi\right)\right) \tag{49}$$

where M_x, M_y, u and v have been defined in Eq. (34) and following. Defining the phase of the mean field φ' as $M_x + iM_y = M\exp(i\varphi')$, the global variable is $\gamma = (u, v, M, \varphi', A, \varphi)$.

Step 2: As remarked in step 2 of Section 2, the contribution to the entropy of the two field variables A, φ, is negligible (of order $1/N$). Hence, the Ψ function reduces to the one of the HMF model, see formula (38). Finally, one obtains the same contributions to the kinetic and configurational entropies, as shown in formulas (41) and (42).

Step 3: Defining the total momentum density as $\sigma = P/N$, the microcanonical variational problem to be solved is

$$S(\varepsilon, \sigma, \delta) = \sup_{\gamma}\left[\frac{1}{2}\ln(u - v^2) + s_{\mathrm{conf}}(M) \,\middle|\, \varepsilon = \frac{u}{2} + 2AM\sin\left(\varphi' - \varphi\right) - \delta A^2,\ \sigma = v + A^2\right]. \tag{50}$$

Using the constraints of the variational problem, one can express u and v as functions of the other variables, obtaining the following form of the entropy

$$S(\varepsilon,\sigma,\delta)=\sup_{A,\varphi,M,\varphi'}\left[\frac{1}{2}\ln\left[2\left(\varepsilon-\frac{\sigma^2}{2}\right)-4AM\sin\left(\varphi'-\varphi\right)+2(\delta-\sigma)A^2-A^4\right]+s_{\mathrm{conf}}(M)\right]. \tag{51}$$

The extremization over the variables φ and φ' is straightforward, since by direct inspection of formula (51), it is clear that the entropy is maximized when $\varphi'-\varphi=-\pi/2$. Then

$$S(\varepsilon,\sigma,\delta)=\sup_{A,M}\left[\frac{1}{2}\ln\left[2\left(\varepsilon-\frac{\sigma^2}{2}\right)+4AM+2(\delta-\sigma)A^2-A^4\right]+s_{\mathrm{conf}}(M)\right]\equiv\sup_{A,M}s(A,M). \tag{52}$$

The non-zero σ case can be reduced to the vanishing σ problem using the identity $S(\varepsilon,\sigma,\delta)=S(\varepsilon-\sigma^2/2,0,\delta-\sigma)$. From now on we will discuss only the zero momentum case, changing $\varepsilon+\sigma^2/2\to\varepsilon$ and $\delta+\sigma\to\delta$. This has also a practical interest, because it is the experimentally relevant initial condition.[38]

The conditions for having a local stationary point are

$$\frac{\partial s}{\partial A}=\frac{2\left(\delta A-A^3+M\right)}{2\varepsilon+2\delta A^2+4AM-A^4}=0, \tag{53}$$

$$\frac{\partial s}{\partial M}=\frac{2A}{2\varepsilon+2\delta A^2+4AM-A^4}-m^{-1}(M)=0, \tag{54}$$

where m^{-1} is defined in formula (46). It is clear that $M=A=0$ is a solution of conditions (53) and (54): it exists only for positive ε. We will limit ourselves to study its stability. It must be remarked that this is the typical initial condition studied experimentally in the FEL: it corresponds to having a beat wave with zero amplitude and the electrons uniformly distributed. The lasing phenomenon is revealed by an exponential growth of both A and the electron bunching parameter M.

The second order derivatives of the entropy $s(A,M)$, computed on this solution, are

$$\frac{\partial^2 s}{\partial A^2}(0,0) = \frac{\delta}{e}, \quad \frac{\partial^2 s}{\partial m^2}(0,0) = -2, \quad \frac{\partial^2 s}{\partial A \partial m}(0,0) = \frac{1}{\varepsilon}. \tag{55}$$

The two eigenvalues of the Hessian are the solutions of the equation

$$x^2 - x\left(-2 + \frac{\delta}{\varepsilon}\right) - \frac{2\delta}{\varepsilon} - \frac{1}{\varepsilon^2} = 0. \tag{56}$$

The stationary point is a maximum if the roots of this equation are both negative. This implies that their sum $\mathcal{S} = (-2 + \delta/\varepsilon)$ is negative and their product $\mathcal{P} = -2\delta/\varepsilon - 1/\varepsilon^2$ is positive. Recalling that we restrict to positive ε values, the condition for the sum to be negative is $\varepsilon > \delta/2$ and the one for the product to be positive is $\varepsilon > -1/(2\delta)$ with $\delta < 0$. The second condition is more restrictive, hence the only region where the solution $M = A = 0$ exists and is stable is $\varepsilon > -1/(2\delta)$ with $\delta < 0$. When crossing the line $\varepsilon = -1/(2\delta)$ ($\delta < 0$), a non-zero bunching solution ($M \neq 0$) originates continuously from the zero bunching one, producing a second order phase transition. This analysis fully coincides with the one performed in the canonical ensemble in ref. 39.

The maximum entropy solution in the region complementary to the one where the zero bunching solution is stable can be obtained[38] by solving numerically Eqs. (53) and (54). This corresponds to having a non-zero field intensity and bunching.

We have not completed in this case the study of the global stability of the different solutions, but we think that, in view of the possibility to map this model exactly onto the HMF model (see Appendix B), no surprise is expected and that the study presented here should fully represent all physical solutions.

4. THE ISING MODEL WITH $1/r^\alpha$ INTERACTIONS

All the models that have been considered above are infinite range: interactions are independent of the distance and the energy can therefore be written *exactly* in terms of global variables. This is no more valid for several important and physically relevant cases. Let us mention in particular the $1/r$ interaction law for gravity and Coulomb systems and the logarithmic interaction for two-dimensional turbulence. A generalized $1/r^\alpha$ interaction has been also introduced and the resulting phase transitions have been analyzed.[40] In all these cases the interaction is singular at short range. Interesting toy models (which generalize the HMF model) without a short distance singularity have been recently proposed.[41–44] In these latter models, XY spins are put on a lattice and interact through

a slowly decreasing non-integrable $1/r^\alpha$ law ($\alpha < d$). For what concerns studies in the microcanonical ensemble, is has been shown[42] that the thermodynamic behavior of these models is independent of the α exponent, after one has adopted an appropriate renormalization of energy and temperature. Salazar *et al.*[45] have studied numerically the problem using microcanonical Monte-Carlo simulations. Besides confirming the scaling properties with α, they have also shown that the number of states is of order $\exp(N)$. The exact solution of these models in the canonical ensemble has been obtained by Campa *et al.*[43] and Vollmayr-Lee and Luijten.[44] The scaling of the magnetization and of the energy curve with the α exponent has been exhibited in full detail.

In this section, we will present a microcanonical solution of the one-dimensional α-Ising model, whose Hamiltonian is given by

$$H_N = \frac{J}{N^{1-\alpha}} \sum_{i>j=1}^{N} \frac{1 - S_i S_j}{|i-j|^\alpha}, \tag{57}$$

where $J > 0$ and spins $S_i = \pm 1$ sit on a one-dimensional lattice with unitary spacing. The $N^{\alpha-1}$ prefactor is introduced in order to have an extensive energy. This model has been first introduced by Dyson[25] and studied for the "integrable" case, $\alpha > 1$, in the canonical ensemble without the $N^{\alpha-1}$ prefactor. We will show that it is possible to obtain an exact microcanonical solution using large deviation theory, when $0 \leqslant \alpha < 1$. This solution can be easily generalized to lattices of larger dimension. In a preliminary paper,[46] a microcanonical solution of this model was presented without rigorously proving the exactness of the mean-field limit.

The study of this model will also give us the opportunity to emphasize the important role played by boundary conditions when the interactions are long range. We will indeed consider both free and periodic boundary conditions. In the latter case, $|i-j|$ is the minimal distance along the circle where one identifies the first and the $(N+1)$th lattice point.

In the solution we will adopt the same scheme described in Section 2.

Step 1: The Hamiltonian H_N cannot be rewritten exactly using a finite dimensional global variable. We overcome this difficulty by defining a coarse-grained function. Let us divide the lattice in K boxes, each with $n = N/K$ sites, and let us introduce the average magnetization in each box m_k, $k = 1, \ldots, K$. In the limit $N \to \infty$, $K \to \infty$, $K/N \to 0$, the magnetization becomes a continuous function $m(x)$, of the $[0, 1]$ interval. After a long but straightforward calculation, described in Appendix C, we can show that it is possible to express H_N as a functional of $m(x)$:

$$H_N = NH[m(x)] + o(N), \tag{58}$$

where

$$H[m(x)] = \frac{J}{2}\int_0^1 \mathrm{d}x \int_0^1 \mathrm{d}y \frac{1 - m(x)m(y)}{|x-y|^\alpha}. \tag{59}$$

The estimation is uniform on all configurations.

Step 2: The probability to get a given magnetization m_k in the kth box from all *a priori* equiprobable microscopic configurations obeys a local large deviation principle $P(m_k) \propto \exp[ns(m_k)]$, with

$$s(m_k) = -\frac{1+m_k}{2}\ln\frac{1+m_k}{2} - \frac{1-m_k}{2}\ln\frac{1-m_k}{2}. \tag{60}$$

Since the microscopic random variables in the different boxes are independent and no global constraints has yet been imposed, the probability of the full global variable $(m_1, \ldots, m_K)$ can be expressed in a factorized form as

$$\begin{aligned} P(m_1, m_2, \ldots, m_K) &= \prod_{i=1}^{K} P(m_i) \simeq \prod_{i=1}^{K} \mathrm{e}^{ns(m_i)} \\ &= \exp\left[nK \sum_{i=1}^{K} \frac{s(m_i)}{K}\right] \simeq \mathrm{e}^{NS[m(x)]}, \end{aligned} \tag{61}$$

where $S[m(x)] = \int_0^1 s(m(x))\,\mathrm{d}x$ is the entropy functional associated to the global variable $m(x)$. Large deviation techniques rigorously justify these calculations,[47] proving that entropy is proportional to N, also in the presence of long-range interactions. This result is independent of the specific model considered; it applies, for instance, also to the long-range XY spin model studied by Salazar *et al.*[45]

Step 3: It is now straightforward to formulate the variational problem in the microcanonical ensemble

$$S(\varepsilon) = \sup_{m(x)} \left(S[m(x)] \mid \varepsilon = H[m(x)]\right). \tag{62}$$

Let us remark that the optimization problem (62) has to be solved in a functional space. In general, this has to be done numerically, taking into account boundary conditions. In this paper, we consider only free

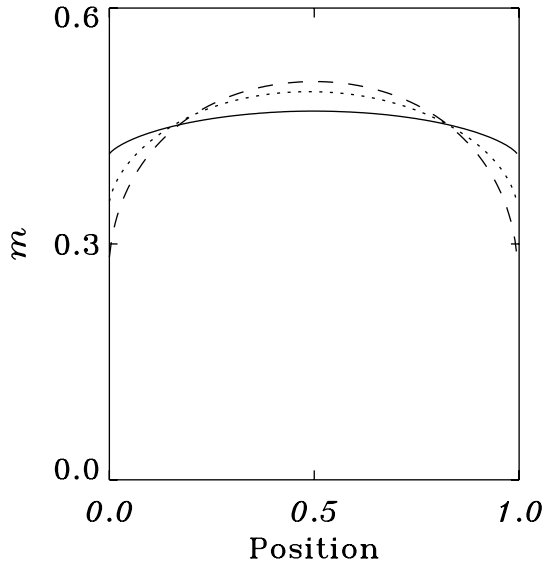

Fig. 4. Equilibrium magnetization profile for the α-Ising model with free boundary conditions at an energy density $\varepsilon = 0.1$ for $\alpha = 0.2$ (solid line), $\alpha = 0.5$ (dotted line) and $\alpha = 0.8$ (dashed line).

and periodic boundary conditions. In the former case, the only available solutions are numerical. An example of a maximal entropy magnetization profile obtained for free boundary conditions is shown in Fig. 4 for different values of α. In the following of this section, we will treat the periodic boundary conditions case, for which analytical result can be obtained.

In the periodic boundary case, the distance $|x-y|$ in the energy (57) is defined as the minimal one on the circle, obtained when the two boundaries of the interval [0, 1] are identified. Both entropy and free energy can be obtained in analytical form for homogeneous magnetization profiles.

In Appendix D, we prove that for $\beta < \beta_c = (1-\alpha)/(J2^{\alpha})$ there is a unique global maximum of S, corresponding to a constant zero magnetization profile. The variational problem (62), where S is defined in Eq. (60), leads to the equation

$$\tanh^{-1}(m(x)) = \beta J \int_0^1 \frac{m(y)}{|x-y|^{\alpha}}\,\mathrm{d}y, \tag{63}$$

where β is a Lagrange multiplier. For $\beta > \beta_c$, we restrict ourselves to solutions with constant magnetization profiles, i.e. $m(x) = m$. We prove in Appendix D that these solutions are locally stable, i.e. close non-constant

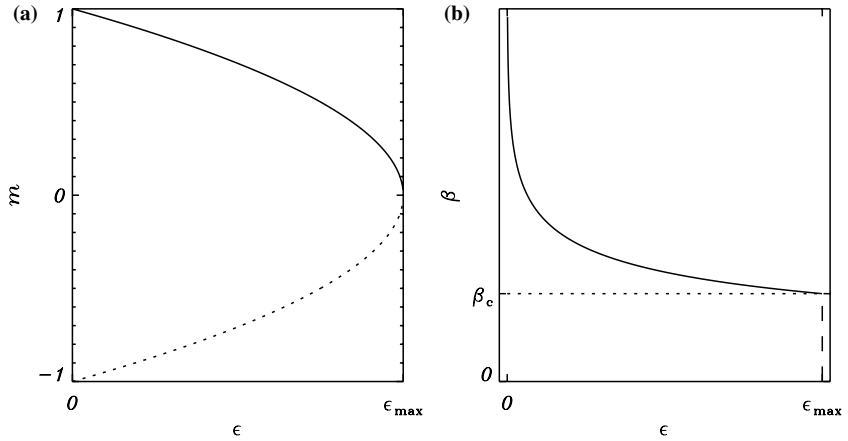

Fig. 5. (a) Equilibrium magnetization in the allowed energy range in the microcanonical ensemble for the α-Ising model with $\alpha = 0.5$; the negative branch is also reported with a dotted line. (b) Inverse temperature versus energy in the microcanonical ensemble (solid line). The canonical ensemble result superposes to the microcanonical one in the interval $[\beta_c, \infty]$ and is represented by a dashed line for $\beta \in [0, \beta_c]$. β_c is then the inverse critical temperature in the canonical ensemble. In the microcanonical ensemble, no phase transition is present.

profiles have a smaller entropy. Moreover, these are the only solutions when $\alpha = 0$, since the right-hand-side of Eq. (63) is then independent of x. For constant profiles, the relation between energy and magnetization is

$$\varepsilon = \varepsilon_{\max}\left(1 - m^2\right), \tag{64}$$

where we have used $\int_0^1 \mathrm{d}x|x-y|^{-\alpha} = 2^\alpha/(1-\alpha)$ and $\varepsilon_{\max} = 1/(2\beta_c)$. Hence, fixing the energy implies fixing the magnetization and, consequently, the Lagrange multiplier β in Eq. (63). Expressing the magnetization in terms of the energy in the entropy formula (60) allows to derive the caloric curve $\beta = dS/d\varepsilon$. The consistency equation (63) has always a non-vanishing magnetization solution in the whole energy range $[0, \varepsilon_{\max}]$: this is reported in Fig. 5(a). The caloric curve is shown in Fig. 5(b) with full line. The limit temperature β_c is attained at zero magnetization, which is a boundary point.

In the canonical ensemble, one has to solve the variational problem (30). This leads to exactly the same consistency equation (63), where the Lagrange multiplier is replaced by the inverse temperature β. Solving this consistency equation on the full positive β axis, one finds a zero magnetization for $\beta < \beta_c$ and non-vanishing one for $\beta > \beta_c$. The caloric curve is

obtained taking the derivative $\varepsilon = dF/d\beta$. The graph of this function is reported in Fig. 5(b) and superposes to the microcanonical caloric curve from infinity down to β_c while it is represented by the dashed line for $\beta < \beta_c$.

It follows that in the region $[0, \beta_c]$, the two ensembles are not equivalent. In this case, a single microcanonical state at $\varepsilon_{\max}$ corresponds to many canonical states with canonical inverse temperatures in the range $[0, \beta_c[$. Thus, in such a case, the canonical inverse temperature is not equal to the microcanonical one. In the microcanonical ensemble, the full high temperature region is absent and, therefore, no phase transition is present or, in other terms, the phase transition is at the boundary of the accessible energy values. The entropy is always concave, hence no inequivalence can be present in the allowed energy range, apart from the boundaries. This situation is called partial equivalence.[19,48] This ensemble inequivalence persists for all α values below one, and is removed only for $\alpha = 1$ when $\varepsilon_{\max} \to \infty$ and $\beta_c \to 0$: the phase transition is not present in both ensembles and the system is always in its magnetized phase.

The main drawback of this analysis is the difficulty to obtain analytical solutions of Eq. (63) for non-constant magnetization profiles, which is the typical situation when boundary conditions are not periodic. However, we have shown that, for periodic boundary conditions, constant magnetization profiles are locally stable (see Appendix D), but the proof of nonexistence of generic magnetization profiles with larger entropy, and hence the global stability analysis, remains to be done.

An advantage of the method we have exposed is its flexibility and applicability to more complex models. For instance, some results of the kind presented here have been already obtained for the α-Blume–Emery–Griffiths model.[9,20]

It is also interesting to check how fast one reaches the $N \to \infty$ solution as one increases the number of spins N. Figure 6 shows entropy density as a function of energy density for the α-Ising model with $\alpha = 0.8$ and periodic boundary conditions. The figure emphasizes that the asymptotic result is already accurate enough for $N = 100$.

5. CONCLUSIONS AND PERSPECTIVES

In this paper, we have discussed examples of the application of large deviation techniques to the study of the statistical mechanics of infinite range models, at equilibrium, in the microcanonical and canonical ensembles. Besides that, we have shown how to construct a mean-field Hamiltonian for the Ising model in one dimension with $1/r^{\alpha}$ interaction $(0 \leqslant \alpha < 1)$. The solution of simple toy models already shows interesting

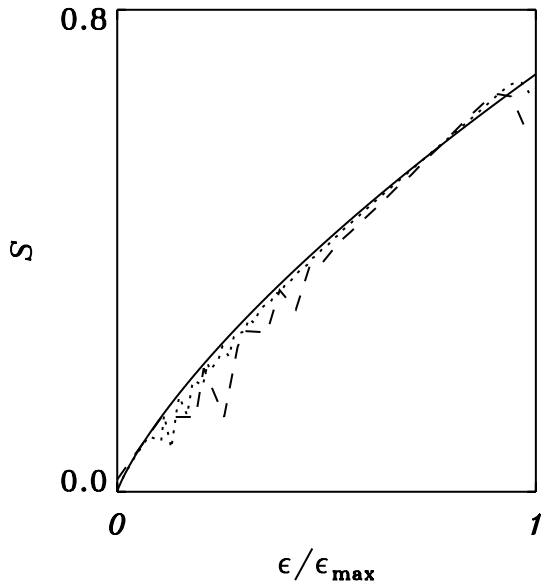

Fig. 6. Entropy density versus energy density for the α-Ising model but with periodic boundary conditions and with $\alpha = 0.8$. The solid curve represents the theoretical solution, whereas the dashed and dotted lines are determined by microcanonical Monte-Carlo simulations with $N = 34$ and $N = 100$, respectively (data provided by R. Salazar).

ensemble inequivalence features, like negative specific heat. Among these simple models, one should point out those with continuous state variables, because the Hamiltonian dynamics becomes accessible and one can then study also non-equilibrium features. Remarkable is also the solution of the Colson–Bonifacio model, which is believed to capture the phenomenology of the saturated state of the free-electron laser.

It is important to emphasize that the method proposed in this paper does not apply to all long-range interacting systems. In particular, those for which statistical mechanics cannot be reduced to a mean-field variational problem are excluded. As presented in Section 2, the method is strongly dependent on the possibility to introduce global or coarse-grained variables: examples are the averaged magnetization, the total kinetic energy, etc. The coarse-grained variables allow one to describe structures whose size is of the order of the total size of the system; however, they may be insufficient to characterize the effect of short-range interaction. A typical example is the Ising model with attractive short-range interactions and repulsive long-range couplings studied by Grousson *et al.*[49] The creation of large scale structures needs an infinite

energy, because of the repulsive long-range component. However, the competition between repulsion and attraction can lead to interesting structures, such as alternating positive and negative magnetized stripes. Indeed, despite the long-range character of the interaction, this system is additive and these structures are therefore compatible with the predicted zero magnetization at large scale. Still in the context of canonical ensemble, worth quoting are the results of Kardar[50] who, analyzing an Ising model with both short-range and long-range interactions was able to derive the exact free energy by a minimization procedure. Obtaining similar results for the microcanonical entropy would be extremely important.

The application of the techniques described in this paper to more realistic N-body systems is an important issue. The extension to wave-particle interactions[6] should not be too difficult. The mean-field description of the two-dimensional point vortices model[51] has been rigorously obtained in a series of papers.[13,52,53] On the contrary, due to the strong short-distance singularity, similar results for self-gravitating systems[2,54] have not been obtained and are a challenging current issue. What is usually done is: (i) in equilibrium, to conjecture the validity of the mean-field description; (ii) out-of-equilibrium, to consider the Vlasov–Poisson equation as a good approximation of the short time dynamics. Once the mean-field description is introduced at finite time (Euler equation, Vlasov–Poisson equation), the statistical mechanics can be derived using large deviation techniques.[18,19] However, it is not equivalent to the original statistical mechanics of the N-body system. Examples of this inequivalence, due to the exchange of the two limits $t \to \infty$ and $N \to \infty$, are given in refs. 8 and 38 for the HMF and the Colson–Bonifacio model.

APPENDIX A. ALTERNATIVE DERIVATION OF THE MICROCANONICAL SOLUTION OF THE HMF MODEL

The microcanonical solution of the HMF model (32) can be alternatively obtained using the traditional method applied for self-gravitating systems.[37] Denoting by K and V kinetic and potential energy, respectively, the number of microscopic configurations corresponding to the energy E is given by

$$\Omega_N(E) = \int \prod_i dp_i d\theta_i \, \delta(E - H_N) \tag{A.1}$$

$$= \int \prod_i dp_i d\theta_i \underbrace{\int dK\, \delta\left(K - \sum_i \frac{p_i^2}{2}\right)}_{=1} \delta\left(E - K - V(\{\theta_i\})\right) \tag{A.2}$$

$$= \int dK \underbrace{\int \prod_i dp_i\, , \delta\left(K - \sum_i \frac{p_i^2}{2}\right)}_{\Omega_{\text{kin}}(K)} \underbrace{\int \prod_i d\theta_i \delta\left(E - K - V(\{\theta_i\})\right)}_{\Omega_{\text{conf}}(E-K)} . \tag{A.3}$$

The factor Ω_{kin} is classical and corresponds to the volume of the hypersphere with radius $R = \sqrt{2K}$ in N dimensions: its expression is $\Omega_{\text{kin}} = 2\pi^{N/2}/\Gamma(1 + N/2)$. Using the asymptotic expression of the Γ-function, $\ln \Gamma(N) \simeq N \ln N - N$, one obtains

$$\Omega_{\text{kin}}(K) \overset{N\to+\infty}{\sim} \exp\left(\frac{N}{2}\left[1 + \ln \pi - \ln \frac{N}{2} + \ln(2K)\right]\right) \tag{A.4}$$

$$= \exp\left(\frac{N}{2}\left[1 + \ln(2\pi) + \ln u\right]\right), \tag{A.5}$$

where $u = 2K/N$. Defining the configurational entropy per particle $s_{\text{conf}}(\widetilde{V}) = (\ln \Omega_{\text{conf}}(N\widetilde{V}))/N$, where $\widetilde{V} = (E - K)/N$, Eq. (A.3) can be rewritten as

$$\Omega_N(\varepsilon N) \overset{N\to+\infty}{\sim} \frac{N}{2} \int du \exp\left[N\left(\frac{1}{2} + \frac{\ln(2\pi)}{2} + \frac{1}{2}\ln u + s_{\text{conf}}(\widetilde{V})\right)\right]. \tag{A.6}$$

Hence, solving the integral in the saddle point approximation, gives the entropy modulo a trivial constant

$$S(\varepsilon) = \lim_{N\to+\infty} \frac{1}{N} \ln \Omega_N(\varepsilon N) \tag{A.7}$$

$$= \frac{1}{2} \sup_u \left[\frac{1}{2}\ln u + s_{\text{conf}}(\widetilde{V})\right] \tag{A.8}$$

to which Eq. (43) reduces once the sup on M is performed. Indeed, this expression of the entropy assumes the knowledge of the configurational entropy s_{conf}, which is determined by solving the extremal condition in Eq. (42), and is restricted to total vanishing momentum $v = 0$. Hence, the method given in the text is slightly more general.

APPENDIX B. MAPPING THE FEL MODEL ONTO HMF

The microcanonical solution of the FEL model (see Eq. (48)) can be expressed in terms of the HMF Hamiltonian using the Laplace representation of the Dirac δ-function and a Gaussian integration. After performing the change of variables $\widetilde{\theta}_i = \theta_i - \varphi$, the microcanonical volume of the FEL is given by

$$\Omega(E) = \iiint \prod_i dp_i d\widetilde{\theta}_i dA\, \delta(E - H_N) \tag{B.1}$$

$$= \iiint \prod_i dp_i d\widetilde{\theta}_i dA\, \frac{1}{2i\pi} \int_\Gamma d\lambda\, \mathrm{e}^{\lambda(E-H_N)}, \tag{B.2}$$

where Γ is a path on the complex λ-plane, going from $-i\infty$ to $+i\infty$, which crosses the real axis at a positive value.

Introducing the FEL Hamiltonian

$$\Omega(E) = \int \prod_i dp_i\, \mathrm{e}^{\lambda\left(E - \sum_{j=1}^N \frac{p_j^2}{2}\right)} \iint \prod_i d\widetilde{\theta}_i dA \times \frac{1}{2i\pi} \int_\Gamma d\lambda\, \mathrm{e}^{\lambda(N\delta A^2 - 2NA\widetilde{M}_y)}, \tag{B.3}$$

and performing the Gaussian integral over the field variable A, one gets

$$\Omega(E) = \int \prod_i dp_i \int \prod_i d\widetilde{\theta}_i \frac{1}{2i\pi} \times \int_\Gamma d\lambda\ \mathrm{e}^{\lambda\left(E - \sum_{j=1}^N \frac{p_j^2}{2} - N\frac{\widetilde{M}_y^2}{\delta} - \frac{1}{2}\ln[\lambda N(-\delta)]\right)} \frac{\sqrt{\pi}}{2} \tag{B.4}$$

$$= \int \prod_i dp_i \int \prod_i d\widetilde{\theta}_i\, \delta\left(E - \sum_{j=1}^N \frac{p_j^2}{2} - N\frac{\widetilde{M}_y^2}{\delta} - \frac{1}{2}\ln[\lambda N(-\delta)]\right) \frac{\sqrt{\pi}}{2}. \tag{B.5}$$

In the large N-limit, one can neglect all constants and the $\ln N$ term in the argument of the Dirac δ, obtaining the microcanonical volume for the Hamiltonian

$$H_N = \sum_{j=1}^N \frac{p_j^2}{2} + N\frac{\widetilde{M}_y^2}{\delta}. \tag{B.6}$$

Hence, for negative values of the parameter δ, solving the microcanonical problem for the FEL Hamiltonian (48) is formally equivalent to obtaining the solution of the HMF Hamiltonian (33) with $C = 2/\delta$ and $M_x = 0$.

APPENDIX C. DERIVATION OF FORMULA (58) FOR THE α-ISING MODEL

Denoting by $\Sigma_N = \{-1, 1\}^N$ the phase space of the α-Ising model, its Hamiltonian is defined as a function of Σ_N to $\mathbb{R}$

$$H_N : \Sigma_N \to \mathbb{R} \tag{C.1}$$

$$\omega_N \mapsto J \sum_{i>j} \frac{1 - S_i S_j}{|i-j|^\alpha}, \tag{C.2}$$

where $\omega_N = (S_1, \ldots, S_N)$ is a given microscopic configuration.

The coarse-graining operator $Y_{N,K}$ divides the lattice into K boxes of size $n = N/K$ and defines a locally averaged magnetization m_k in the kth box B_k. The coarse-grained magnetization is then a step function, which takes a constant value

$$m_k = \frac{1}{n} \sum_{i \in B_k} S_i, \tag{C.3}$$

in B_k. It is convenient to introduce the operator

$$Y_{N,K} : \Sigma_N \to L^2([0, 1]), \tag{C.4}$$

which maps the configuration space to the coarse-grained magnetization. The length of the lattice is then renormalized to the interval $[0, 1]$ and, in the limit $N \to \infty$, this operator defines a continuous magnetization profile $m(x)$. The limit of the number of boxes $K \to \infty$ is taken in such a way that the number of sites per box diverges $N/K \to \infty$, as already mentioned in the text. In the following, we will use free boundary conditions (The choice of periodic boundary conditions would change only some details of the calculation).

The energy as a function of the coarse-grained magnetization is defined as

$$\widetilde{h}[Y_{N,K}(\omega_N)] = \sum_{k,l=1}^{K} \frac{J}{2} (1 - m_k m_l)\, d_{kl}, \tag{C.5}$$

where

$$d_{kl} = \int_{(k-1)/K}^{k/K} \int_{(l-1)/K}^{l/K} \mathrm{d}x\, dy \frac{1}{|x-y|^{\alpha}}. \tag{C.6}$$

Hence, the composition of the operator $Y_{N,K}$ with the functional $\widetilde{h}$ allows to define a map, which associates to each microscopic configuration $\omega_N \in \Sigma_N$ a given energy. Our aim is to find a series $K(N)$ such that

$$\lim_{N\to\infty} \sup_{\omega_N \in \Sigma_N} \left| \frac{H_N(\omega_N)}{N^{2-\alpha}} - \widetilde{h}[Y_{N,K(N)}(\omega_N)] \right| = 0. \tag{C.7}$$

This is what we mean by uniform convergence of the Hamiltonian $H_N(\omega_N)$ to its functional form $H[m(x)]$, defined in formula (59).

The proof relies on the long-range character of the interaction ($0 \leqslant \alpha < 1$). It is straightforward but lengthy.

Let us first express $\widetilde{h}[Y_{N,K(N)}(\omega_N)]$ directly as a function of the spin variables S_i

$$\widetilde{h}[Y_{N,K(N)}(\omega)] = \sum_{k,l=1}^{K} \frac{d_{kl}}{n^2} \sum_{\substack{i\in B_k \\ j\in B_l}} \frac{J}{2}(1 - S_i S_j). \tag{C.8}$$

In order to compare expression (C.8) with $H_N/N^{2-\alpha}$, let us first introduce the reduced Hamiltonian

$$g_{N,K} = \frac{1}{N^{2-\alpha}} \sum_{\substack{k,l=1 \\ l\neq k}}^{K} \sum_{\substack{i\in B_k \\ j\in B_l}} \frac{J}{2} \frac{(1 - S_i S_j)}{|nk - nl|^{\alpha}}, \tag{C.9}$$

which is in fact the original Hamiltonian $H_N/N^{2-\alpha}$ where the distance between two sites is approximated by the distance among the boxes to which they belong. Using the triangular inequality, one gets

$$\begin{aligned} \left| \frac{H_N(\omega_N)}{N^{2-\alpha}} - \widetilde{h}[Y_{N,K(N)}(\omega_N)] \right| &\leqslant \left| \frac{H_N(\omega_N)}{N^{2-\alpha}} - g_{N,K} \right| \\ &+ \left| g_{N,K} - \widetilde{h}[Y_{N,K(N)}(\omega_N)] \right| \equiv A + B. \end{aligned} \tag{C.10}$$

We will show how both A and B can be bounded from above by quantities which vanish when $N \to \infty$, under the hypothesis that $0 \leqslant \alpha < 1$.

C.1. Upper Bound of A

Let us first rewrite $H_N/N^{2-\alpha}$ as a sum of two terms: the first contains contributions from sites which belong to different boxes, the second from those which are in the same box,

$$\frac{H_N}{N^{2-\alpha}} = \frac{1}{N^{2-\alpha}} \sum_{\substack{k,l=1 \\ l\neq k}}^{K} \sum_{\substack{i\in B_k \\ j\in B_l}} \frac{J}{2} \frac{(1-S_iS_j)}{|i-j|^\alpha} + \frac{1}{N^{2-\alpha}} \sum_{k=1}^{K} \sum_{i,j\in B_k} \frac{J}{2} \frac{(1-S_iS_j)}{|i-j|^\alpha}. \tag{C.11}$$

Then

$$A \leqslant \frac{1}{N^{2-\alpha}} \left| \sum_{\substack{k,l=1 \\ l\neq k}}^{K} \sum_{\substack{i\in B_k \\ j\in B_l}} \frac{J}{2}(1-S_iS_j) \left(\frac{1}{|i-j|^\alpha} - \frac{1}{|nk-nl|^\alpha} \right) \right| + \left| \frac{1}{N^{2-\alpha}} \sum_{k=1}^{K} \sum_{i,j\in B_k} \frac{J}{2} \frac{(1-S_iS_j)}{|i-j|^\alpha} \right| \equiv A_1 + A_2. \tag{C.12}$$

The bound of A_2 is easy to find since $J(1-S_iS_j)/2 \leqslant J$ and $|i-j|^\alpha \geqslant 1$ for $\alpha \in [0, 1]$. One obtains

$$A_2 \leqslant J \frac{Kn^2}{N^{2-\alpha}} = J \frac{N^\alpha}{K}. \tag{C.13}$$

This quantity vanishes in the large N limit if K diverges faster than N^α (and certainly slower than N). This is the first point where the long-range nature of the interaction is used.

In order to bound A_1 let us divide the first sum in formula (C.12) into three parts : $k-l>1$, $k-l<-1$ and $|k-l|=1$. The last part, $|k-l|=1$, can be bounded from above by $2JN^\alpha/K$, which vanishes in the large N limit. The two remaining parts are symmetric, hence we treat only the case $k-l>1$. Since $i\in B_k$ and $j\in B_l$, this implies that $n(k-l-1)<i-j<n(k-l+1)$. Hence,

$$\frac{1}{n^\alpha} \frac{1}{(k-l+1)^\alpha} < \frac{1}{|i-j|^\alpha} < \frac{1}{n^\alpha} \frac{1}{(k-l-1)^\alpha}. \tag{C.14}$$

Substracting $1/|nk-nl|^\alpha$, one gets

$$\frac{1}{n^\alpha}\left(\frac{1}{(k-l+1)^\alpha}-\frac{1}{(k-l)^\alpha}\right)<\frac{1}{|i-j|^\alpha}-\frac{1}{n^\alpha(k-l)^\alpha}<\frac{1}{n^\alpha}\left(\frac{1}{(k-l-1)^\alpha}-\frac{1}{(k-l)^\alpha}\right). \tag{C.15}$$

This leads to

$$\left|\frac{1}{|i-j|^\alpha}-\frac{1}{n^\alpha(k-l)^\alpha}\right|<\frac{1}{n^\alpha}\left(\frac{1}{(k-l-1)^\alpha}-\frac{1}{(k-l)^\alpha}\right). \tag{C.16}$$

Thus

$$\frac{1}{N^{2-\alpha}}\sum_{\substack{k,l=1\\k-l>1}}^{K}\sum_{\substack{i\in B_k\\j\in B_l}}\left|\frac{1}{|i-j|^\alpha}-\frac{1}{n^\alpha(k-l)^\alpha}\right|$$

$$<\frac{1}{N^{2-\alpha}}\frac{n^2}{n^\alpha}\times\sum_{\substack{k,l=1\\k-l>1}}^{K}\left[\frac{1}{(k-l-1)^\alpha}-\frac{1}{(k-l)^\alpha}\right] \tag{C.17}$$

$$=\frac{n^{2-\alpha}}{N^{2-\alpha}}\sum_{k=3}^{K}\sum_{l=1}^{k-2}\left[\frac{1}{(k-l-1)^\alpha}-\frac{1}{(k-l)^\alpha}\right] \tag{C.18}$$

$$=\frac{1}{K^{2-\alpha}}\sum_{k=3}^{K}\left[1-\frac{1}{(k-1)^\alpha}\right]<\frac{K}{K^{2-\alpha}}. \tag{C.19}$$

Hence, this part of A_1 is bounded by $JK^{\alpha-1}$, which vanishes in the large N limit. The symmetric part of $A_1 k-l<-1$ can be treated exactly in the same way.

C.2. Upper Bound of B

Dividing the sum in two parts, one for sites in different boxes and the other for sites in the same box, and using the triangular inequality, one gets

$$B \leqslant \frac{1}{N^{2-\alpha}} \left| \sum_{\substack{k,l=1 \\ l\neq k}}^{N} \sum_{\substack{i\in B_k \\ j\in B_l}} \frac{J}{2}(1-S_i S_j)\left(\frac{1}{|nk-nl|^{\alpha}} - \frac{d_{kl}}{n^2}\right)\right| + \left| \sum_{k} \frac{d_{kk}}{n^2} \sum_{i,j\in B_k} \frac{J}{2}(1-S_i S_j)\right| \equiv B_1 + B_2. \tag{C.20}$$

In order to estimate the size of B_2, one has first to evaluate $\sum_k d_{kk}$. Indeed,

$$\begin{aligned} d_{kl} &= \int_0^{1/K}\int_0^{1/K} \mathrm{d}x\, dy \frac{1}{|x-y+\frac{k-l}{K}|^{\alpha}} \\ &= \frac{1}{K^{2-\alpha}} \int_0^1 \int_0^1 du\, dv \frac{1}{|u-v+k-l|^{\alpha}}. \end{aligned} \tag{C.21}$$

Therefore $\sum_k d_{kk} \sim K^{\alpha-1}$. Hence, $B_2 \leqslant J K^{\alpha-1}$, which vanishes in the large N-limit.

For what B_1 is concerned, exchanging the modulus with the sums and using the expression for d_{kl} (formula (C.21)), one obtains

$$\begin{aligned} B_1 &\leqslant J \sum_{\substack{k,l=1 \\ l\neq k}}^{N} \left| \frac{n^2}{N^{2-\alpha} n^{\alpha} |k-l|^{\alpha}} - d_{kl}\right| \\ &\leqslant J \sum_{\substack{k,l=1 \\ l\neq k}}^{N} \frac{1}{K^{2-\alpha}} \left| \int_0^1 \int_0^1 du\, dv \frac{1}{|u-v+k-l|^{\alpha}} - \frac{1}{|k-l|^{\alpha}}\right|. \end{aligned} \tag{C.22}$$

Similarly as for A_1, one divides the sum in three parts $k-l>1$, $k-l<-1$ and $|k-l|=1$. The last part gives a term of order $J K^{\alpha-1}$, which vanishes in the large N limit. If $k-l>1$, analogously to Eq. (C.15), one obtains

$$\frac{1}{(k-l+1)^\alpha} - \frac{1}{(k-l)^\alpha} < \int_0^1 \int_0^1 du\, dv \frac{1}{|u-v+k-l|^\alpha} - \frac{1}{|k-l|^\alpha} < \frac{1}{(k-l-1)^\alpha} - \frac{1}{(k-l)^\alpha}, \tag{C.23}$$

which leads to

$$\left| \int_0^1 \int_0^1 du\, dv \frac{1}{|u-v+k-l|^\alpha} - \frac{1}{|k-l|^\alpha} \right| < \frac{1}{(k-l-1)^\alpha} - \frac{1}{(k-l)^\alpha}. \tag{C.24}$$

Summing this term over k and l gives again a factor of order K. Then, this part is also bounded from above by a factor $JK^{\alpha-1}$. The symmetric part $k-l<1$ is equally treated.

All terms in B are bounded by $JK^{\alpha-1}$, and therefore vanish in the large N limit. This concludes the proof of formula (C.7) and assures that $\tilde{h}$ converges to H.

We would like to emphasize that throughout of this derivation, the only place where we use the Ising interaction of the model is where we bound $J(1-S_iS_j)/2$ by J. It is then easy to realize that the method can be generalized to other models like Potts, Blume–Emery–Griffiths, XY, with spatially decaying interactions. On the contrary, the presence of the lattice is crucial, because it avoids microscopic configurations where the state variables concentrate on single point, leading to a divergence.

APPENDIX D. PROOF OF STABILITY OF CONSTANT MAGNETIZATION PROFILES FOR THE α-ISING MODEL WITH PERIODIC BOUNDARY CONDITIONS

We prove here the stability of constant magnetization profiles for the α-Ising model in the context of the canonical ensemble. This also implies stability in the microcanonical ensemble. Let us consider the free energy $F[m(x)]$ as a functional of $m(x)$

$$F[m(x)] = -S[m(x)] + \beta H[m(x)], \tag{D.1}$$

where the entropy functional $S[m(x)]$ is defined in formula (61). We will limit ourselves to periodic boundary conditions. Let us study the second variation of F

$$\delta^2 F(m(x)) = -\int_0^1 \mathrm{d}x\, s''[m(x)]\, \delta m(x)^2 - \beta \frac{J}{2} \int_0^1 \mathrm{d}x \int_0^1 dy \frac{\delta m(x) \delta m(y)}{|x-y|^\alpha}, \tag{D.2}$$

where s'' is the second derivative of s. Let us express the variation $\delta m(x)$ in Fourier components

$$\delta m(x) = \sum_{k=-\infty}^{+\infty} \delta m_k e^{2i\pi kx}, \tag{D.3}$$

and define

$$c_k^\alpha = \int_0^1 dx \ \frac{e^{2i\pi kx}}{|x-y|^\alpha} = 2\int_0^{1/2} dx \frac{\cos(2\pi kx)}{|x|^\alpha}, \tag{D.4}$$

where, since we consider periodic boundary conditions, $|\cdot|$ denotes the distance on the circle. Using the inequality $s''(m(x)) \leqslant s''(0)$ and replacing the Fourier expansion (D.3) in Eq. (D.2), we obtain

$$\delta^2 F(m(x)) \geqslant \sum_{k=-\infty}^{+\infty} \left(-s''(0) - \beta \frac{J}{2} c_k^\alpha\right) \delta m_k^2. \tag{D.5}$$

Remarking that all coefficients c_k^α are positive reals and that for all k, $c_k^\alpha \leqslant c_0^\alpha = 2^\alpha/(1-\alpha)$, one can bound from above all the coefficients in the Fourier sum (D.5) by $(-s''(0) - \beta J c_0^\alpha/2)$.

Thus for $\beta < -2s''(0)/(Jc_0^\alpha) = \beta_c$, one has $\delta^2 F(m(x)) > 0$. In such a case, the free energy is strictly convex, and hence its minimum is unique. This proves the global stability of the state $m(x) = 0$.

For $\beta > \beta_c$, we do not study global stability. Let us however show the local stability of the uniform magnetization state $m(x) = m$. Using Eq. (D.2), one has

$$\delta^2 F(m(x)) \geqslant \sum_{k=-\infty}^{+\infty} \left(-s''(m) - \beta \frac{J}{2} c_k^\alpha\right) \delta m_k^2. \tag{D.6}$$

Using again the property $c_k^\alpha \leqslant c_0^\alpha$, we note that all the Fourier coefficients of Eq. (D.6) are bounded from above by $-s''(m) - \beta J c_0^\alpha/2$. Observing that this latter expression is the second variation of the free energy for uniform magnetization profiles, i.e. $(1-m^2(\beta))^{-1} - \beta/\beta_c$, the analysis of Section 4 implies that this quantity is non negative both for $m \neq 0$ and $\beta > \beta_c$ and for $m = 0$ and $\beta \leqslant \beta_c$. This proves that close to a constant magnetization profile, there is no non-uniform magnetization profile which gives a smaller free energy functional $F[m(x)]$.

ACKNOWLEDGMENTS

We would like to thank J. Michel for very helpful advices, R. Salazar for providing us the numerical data used in Fig. 6 and A. Alastuey, A. Antoniazzi, P. Cipriani and H. Touchette for discussions. This work has been partially supported by the French Ministère de la Recherche grant ACI jeune chercheur-2001 No. 21–31 and the Région Rhône-Alpes for the fellowship No. 01-009261-01. It is also part of the contract COFIN03 of the Italian MIUR *Order and chaos in nonlinear extended systems*. Work at Los Alamos National Laboratory is supported by the US Department of Energy.

REFERENCES

1. T. Dauxois, S. Ruffo, E. Arimondo, and M. Wilkens (eds.), *Dynamics and Thermodynamics of Systems with Long-Range Interactions*, Lecture Notes in Physics, Vol. 602 (Springer, 2002).
2. T. Padmanabhan, *Phys. Rep.* **188**:285 (1990).
3. D. C. Brydges and P. A. Martin, *J. Stat. Phys.* **96**:1163 (1999).
4. P. H. Chavanis, Statistical mechanics of two-dimensional vortices and Stellar systems, in Ref. [1].
5. Y. Elskens, Kinetic theory for plasmas and wave-particle Hamiltonian dynamics, in Ref. [1].
6. Y. Elskens and D. Escande, *Microscopic Dynamics of Plasmas and Chaos* (IOP Publishing, Bristol, 2002).
7. P. Gaspard, *Phys. Rev. E* **68**:056209 (2003).
8. Y. Y. Yamaguchi, J. Barré, F. Bouchet, T. Dauxois, and S. Ruffo, *Physica A* **337**:36 (2004).
9. J. Barré, D. Mukamel, and S. Ruffo, Ensemble inequivalence in mean-field models of magnetisms, in Ref. [1].
10. For short-range interactions, the limit is performed by letting both the number of particles and volume go to infinity, with a fixed ratio between the two quantities.
11. J. Messer and H. Spohn, *J. Stat. Phys.* **29**:561 (1982).
12. P. Hertel and W. Thirring, *Ann. Phys.* **63**:520 (1971) and references therein.
13. M. K. H. Kiessling and J. L. Lebowitz, *Lett. Math. Phys.* **42**:43 (1997) and references therein.
14. J. Barré, D. Mukamel, and S. Ruffo, *Phys. Rev. Lett.* **87**:030601 (2001).
15. D. H. E. Gross, *Microcanonical Thermodynamics: Phase Transitions in Small Systems*, Lecture Note in Physics, Vol. 66, (World Scientific, Singapore, 2001).
16. R. S. Ellis, *Entropy, Large Deviations, and Statistical Mechanics* (Springer-Verlag, New York, 1985).
17. A. Dembo and O. Zeitouni, *Large Deviations Techniques and their Applications* (Springer-Verlag, New York, 1998).
18. J. Michel and R. Robert, *Comm. Math. Phys.* **159**:195 (1994); R. Robert, *Comm. Math. Phys.* **212**:245 (2000).
19. R. S. Ellis, *Physica D* **133**:106 (1999); R. S. Ellis, K. Haven, and B. Turkington, *J. Stat. Phys.* **101**:999 (2000) and *Nonlinearity* **15**:239 (2002).
20. J. Barré, *Mécanique statistique et dynamique hors équilibre de systèmes avec intéractions à longues portées*, PhD thesis (ENS Lyon, 2003).
21. R. S. Ellis, H. Touchette, and B. Turkington, *Physica A* **335**:518 (2004).

22. T. Dauxois, V. Latora, A. Rapisarda, S. Ruffo, and A. Torcini, The Hamiltonian mean field model: From dynamics to statistical mechanics and back, in Ref. [1].
23. M. Antoni and S. Ruffo, *Phys. Rev. E* **52**:2361 (1995).
24. R. Bonifacio, F. Casagrande, G. Cerchioni, L. De Salvo Souza, P. Pierini, and N. Piovella, *Riv. Nuovo Cimento* **13**:1 (1990).
25. F. J. Dyson, *Comm. Math. Phys.* **12**:91 (1969).
26. J. Miller, *Phys. Rev. Lett.* **65**:2137 (1990).
27. R. Robert, and J. Sommeria, *J. Fluid. Mech.* **229**:291 (1991).
28. I. Ispolatov, E. G. D. Cohen, *Physica A* **295**:475 (2001).
29. D. H. E. Gross and E. V. Votyakov, *Eur. Phys. J. B* **15**:115 (2000).
30. Alternatively, one could have left energy non-extensive and accordingly rescale temperature.
31. F. Bouchet and J. Barré, Classification of phase transitions and ensemble inequivalence in systems with long-range interactions, *J. Stat. Phys.* **118**(5–6):1073–1105 (2005).
32. R. Toral, *J. Stat. Phys.* **114**:1393 (2004).
33. C. Anteneodo, *Physica A* **342**:112 (2004).
34. M. Antoni, H. Hinrichsen, and S. Ruffo, *Chaos Soliton and Fractals* **13**:393 (2002).
35. L. Velazquez, R. Sospedra, J. C. Castro, and F. Guzman, On the dynamical anomalies in the Hamiltonian Mean Field model, *cond-mat/0302456*.
36. F. Bouchet, *Phys. Rev. E* **70**:036113 (2004).
37. J. Binney and S. Tremaine, *Galactic Dynamics* (Princeton Series in Astrophysics, 1987).
38. J. Barré, T. Dauxois, G. De Ninno, D. Fanelli, and S. Ruffo, *Physical Review E* **69**:045501 (2004).
39. M. C. Firpo and Y. Elskens, *Phys. Rev. Lett.* **84**:3318 (2000).
40. I. Ispolatov and E. G. D. Cohen, *Phys. Rev. Lett.* **87**:210601 (2000); *Phys. Rev. E* **64**:056103 (2000).
41. C. Anteneodo and C. Tsallis, *Phys. Rev. Lett.* **80**:5313 (1998).
42. F. Tamarit and C. Anteneodo, *Phys. Rev. Lett.* **84**:208 (2000).
43. A. Campa, A. Giansanti, and D. Moroni, *Phys. Rev. E* **62**:303 (2000); *Chaos, Solitons, Fractals* **13**:407 (2002); *J. Phys.* A **36**:6897 (2003).
44. B. P. Vollmayr-Lee and E. Luijten, *Phys. Rev. E* **63**:031108 (2001).
45. R. Salazar, R. Toral, and A. R. Plastino, *Physica A* **305**:144 (2002).
46. J. Barré, *Physica A* **305**:172 (2002).
47. C. Boucher, R. S. Ellis, and B. Turkington, *Ann. Prob.* **27**:297 (1999). Erratum, *Ann. Prob.* **30**:2113 (2002).
48. M. Kastner, submitted to *Phys. Rev. Lett.*; also cond-mat/0412199.
49. M. Grousson, G. Tarjus, and P. Viot, *Phys. Rev. E* **62**:7781 (2000).
50. M. Kardar, *Phys. Rev. B* **28**:244 (1983); *Phys. Rev. Lett.* **51**:523 (1983).
51. L. Onsager, *Nuovo Cimento Suppl.* **6**:279 (1949).
52. M. K. H. Kiessling, *Comm. Pure App. Math.* **46**:27 (1993).
53. E. Caglioti, P. L. Lions, C. Marchioro, and M. Pulvirenti, *Comm. Math. Phys.* **143**:501 (1992); *Comm. Math. Phys.* **174**:229 (1995).
54. D. Lynden-Bell and R. Wood, *Monthly Notices of the Royal Astronomical Society* **138**:495 (1968).